Geomechanics and Engineering, *Vol. 23, No. 1 (2020) 61-69*
DOI: https://doi.org/10.12989/gae.2020.23.1.061

Energy analysis-based core drilling method for the prediction of rock uniaxial compressive strength

Wang Qi*[1,2], Xu Shuo[1,2], Gao Hong Ke[1,2], Zhang Peng[1,2], Jiang Bei[1,2,3] and Liu Bo Hong[1,2]

[1]*State Key Laboratory for Geo-mechanics and Deep Underground Engineering, China University of Mining & Technology (Beijing), Beijing 100083, China*
[2]*Research Center of Geotechnical and Structural Engineering, Shandong University, Jinan 250061, China*
[3]*School of Civil Engineering and Architecture, University of Jinan, Jinan 250022, China*

(Received February 22, 2019, Revised August 5, 2020, Accepted September 10, 2020)

Abstract. The uniaxial compressive strength (UCS) of rock is a basic parameter in underground engineering design. The disadvantages of this commonly employed laboratory testing method are untimely testing, difficulty in performing core testing of broken rock mass and long and complicated onsite testing processes. Therefore, the development of a fast and simple in situ rock UCS testing method for field use is urgent. In this study, a multi-function digital rock drilling and testing system and a digital core bit dedicated to the system are independently developed and employed in digital drilling tests on rock specimens with different strengths. The energy analysis is performed during rock cutting to estimate the energy consumed by the drill bit to remove a unit volume of rock. Two quantitative relationship models of energy analysis-based core drilling parameters (ECD) and rock UCS (ECD-UCS models) are established in this manuscript by the methods of regression analysis and support vector machine (SVM). The predictive abilities of the two models are comparatively analysed. The results show that the mean value of relative difference between the predicted rock UCS values and the UCS values measured by the laboratory uniaxial compression test in the prediction set are 3.76 MPa and 4.30 MPa, respectively, and the standard deviations are 2.08 MPa and 4.14 MPa, respectively. The regression analysis-based ECD-UCS model has a more stable predictive ability. The energy analysis-based rock drilling method for the prediction of UCS is proposed. This method realized the quick and convenient in situ test of rock UCS.

Keywords: core drilling; energy analysis; drilling parameter; rock; uniaxial compressive strength; relationship model; prediction method

1. Introduction

The uniaxial compressive strength (UCS) of rock is an important index that reflects the mechanical properties of rock. Its accurate measurement is a prerequisite for the classification of surrounding rocks and the design and optimization of parameters of the support structure. Currently, a laboratory uniaxial compression test is a common method that is applied to obtain the rock UCS (Chai *et al.* 2019, Zhang *et al.* 2019, Wang and Aladejare 2016, Zhao *et al.* 2015, Kahraman and Yeken 2010). With this method, rock specimens are sampled in the field and transported them to a laboratory for cutting and grinding. The testing cycle is long, and the rock UCS at the project site cannot be obtained in a timely manner. Since the specimens in a laboratory uniaxial compression test are relatively intact, the measured UCS values are typically higher than the in situ values at the project site and cannot accurately reflect the practical parameters of the surrounding rocks at the project site. Especially for underground projects with complex conditions, such as high ground stress (Wang *et al.* 2020b, 2018b), extremely soft rock (Wang *et al.* 2017) and the fault fracture zone (Wu *et al.* 2018, Yong *et al.* 2018), the surrounding rock is loose and fractured after the excavation of the cavern (Yu *et al.* 2020, Wang *et al.* 2018a, Qian *et al.* 2017, Su *et al.* 2017, Langford *et al.* 2016, Arora and Mishra 2015, Kun and Onargan 2013), which hinders the ability to obtain a high-quality core. Therefore, the development of an in situ UCS testing method that is convenient and efficient for field use is necessary.

Many scholars have studied the in situ UCS testing method. Heidari *et al.* (2012) carry out point load tests for cores prepared from the gypsum rocks, and establish the relationships between the point load strength index and UCS to forecast UCS of gypsum rocks, providing a method for indirect prediction of uniaxial compressive strength of rock mass in situ. Momeni *et al.* (2015) conduct tests including point load index test, Schmidt hammer rebound test, p-wave velocity test and dry density test, and develop a particle swarm optimization-based artificial neural network predictive model of UCS. Vyacheslav (2018) get the uniaxial compressive strength of carbonate rocks determined by a standard Schmidt hammer. Kilic and Teymen (2008) perform nondestructive measurement of

*Corresponding author, Professor
E-mail: chinawangqi@163.com

ISSN: 2005-307X (Print), 2092-6219 (Online)

parameters such as Shore hardness index, sound velocity, point load index, porosity, and Schmidt hardness to estimate UCS. Li and Tan (2016) put forward a UCS prediction formula based on P-wave modulus by using the linear fitting method, according to the test data of rock dry density, P-wave velocity and UCS from dacite-porphyrite and shale. Based on the above research, it is cleared that methods such as the point load method and Schmidt hammer testing are popular in situ methods for measuring the rock strength. These types of methods can be employed to measure the strength of a rock mass on a chamber surface. However, for a rock mass located at a considerable depth, surrounding rock core need to be collected for rock strength measurement. Some researchers investigated rock UCS in situ forecast via parameters such as longitudinal wave velocity and density. It needs to be tested after drilling the surrounding rock, and the process is complicated. Therefore, most of the existing in site rock UCS testing methods need to be drilled in advance. If the in site rock UCS can be obtained during drilling, it will simplify the testing process and shorten the testing time.

Digital drilling tests are an effective method to monitor drilling parameters during drilling process such as drilling rate, rotational speed, drilling torque, drilling thrust and so on, which can quantitative control some of these parameters. (Wang *et al.* 2020a, Kalantari *et al.* 2018, Ghosh *et al.* 2018, Zhou *et al.* 2017, Munoz *et al.* 2016). Numerous field and laboratory drilling studies have shown that drilling parameters are closely related to the rock mechanics parameters. Mostofi *et al.* (2011) propose an equation which correlates drilling parameters with formation strength in order to estimate formation strength. Yaşar *et al.* (2011) carry out laboratory drilling test and propose the relationship between UCS and the specific energies for the purpose of determination for UCS of rock. Kumar *et al.* (2011) develop UCS prediction model and investigate the relationships between sound level produced during drilling and physical properties such as uniaxial compressive strength. Wang *et al.* (2019) presents a method for determining rock mechanics parameters using drilling parameters obtained during a field drilling experiment.

Based on the quantitative relationship between the drilling parameters and the UCS, the rock UCS can be quickly acquired during the surrounding rock drilling process using digital drilling technology. Using core drilling, the core can be obtained, and a rock mechanical test can be performed to obtain the test value of rock UCS. The tested UCS can be compared with the predicted UCS for validation to continuously revise the quantitative relationship of the drilling parameters and rock UCS and achieve extensive applicability of the relationship. Therefore, a digital core drilling test is an effective technical means for quick in situ acquisition of the UCS for surrounding rock.

In order to achieve fast and convenient on-site acquisition of rock UCS, the quantitative relationship model between the rock UCS and digital core drilling parameters should be established. Additionally, the digital drilling testing system matching with the relationship model should be developed. Therefore, the key is to establish the relationship model. For this purpose, the core drilling tests and uniaxial compression tests on sandstone and cement mortar specimens of different strengths are conducted, based on the self-developed multi-function digital rock drilling testing system. The energy analysis is performed during rock cutting to get the energy required to drill cut a unit volume of rocks η_c. The energy analysis-based quantitative relationship model of the core drilling parameters and rock UCS (the ECD-UCS model) is established and validated. The energy analysis-based rock drilling method for the prediction of UCS is proposed.

2. Core drilling tests

2.1 Test equipment

The multi-function rock mass digital drilling test system (Fig. 1) developed by the authors is employed for the rock core drilling tests. This system consists of a drilling system, a loading system, a pressure chamber and a monitoring and control system. During the drilling process, the system can provide a maximum drilling thrust of 50 kN, a maximum drilling torque of 400 N·m, and a maximum rotational speed of 400 r/min. The drilling rate (V), rotational speed (N), drilling thrust (F) and drilling torque (M) can be monitored and controlled in real time by the displacement sensor, rotational speed sensor, pressure sensor and torque sensor. The control mode of constant V-N is adopted.

To render the analysis of the rock cutting force more realistic and to accurately establish the quantitative relationship between the drilling parameters and the rock UCS, this study use the polycrystalline diamond compact (PDC) core bit that is developed for digital drilling by the authors. This drill bit (Fig. 1) uses a rectangular PDC sheet to form a cutting edge, which can effectively separate the core and rock mass.

2.2 Test plan

There is a great deal of research indicating that the rock mechanical properties can be reflected by the mechanical test of mortar specimen, which is the rock-like material (Lei *et al.* 2020, Li *et al.* 2016, Zhang *et al.* 2015). In order to carry out the digital core drilling test of the rock with different strengths, the cement mortar and sandstone are adopted to make test specimens with different strengths. The cement mortar specimens with 7 different strength grades are made by changing the proportion of cement, as shown in Table 1. There are 3 groups of specimens for each strength grade, and 21 groups of cement mortar specimens in total. The curing period of cement mortar specimens is 28d at 20°C. All sandstone specimens are intact rocks, with a total of 3. The dimension of the specimens is length × width × height = 150 mm × 150 mm × 200 mm.

The core drilling tests adopt a constant V and N to monitor F and M. V is set to one of two levels: 60 mm/min and 85 mm/min, N is set to one of two levels: 50 r/min and 100 r/min. Sandstone specimens are denoted by "S". Cement mortar specimens of seven strength grades are denoted by "A1"-"A7". The core drilling depth is 120 mm for all specimens. The specific test design is shown in Table 2.

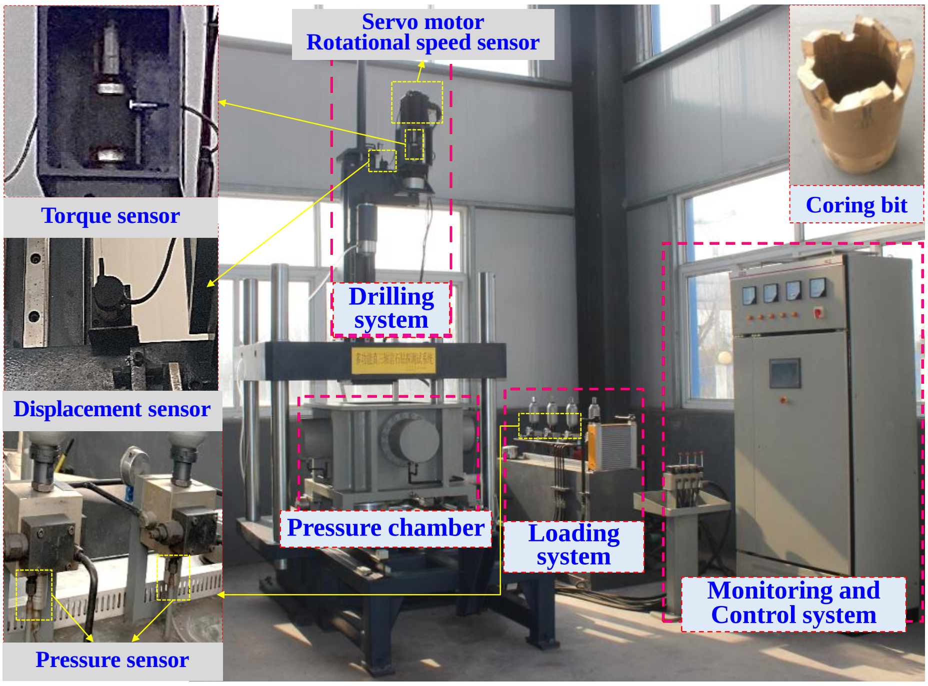

Fig. 1 Multi-function digital rock drilling and testing system

Table 1 Material mix ratios of cement mortar specimens with different strength grades

Strength grade of cement mortar	Cement kg/m^3	Sand kg/m^3	Water kg/m^3
A1	200		
A2	300		
A3	400		
A4	500	1450	300
A5	600		
A6	700		
A7	800		

Table 2 Design of the core drilling test

No. of specimens	V (mm/min)	N (r/min)	No. of specimens	V (mm/min)	N (r/min)
A11	60	50	A21	60	50
A12	60	100	A22	60	100
A13	85	100	A23	85	100
A31	60	50	A41	60	50
A32	60	100	A42	60	100
A33	85	100	A43	85	100
A51	60	50	A61	60	50
A52	60	100	A62	60	100
A53	85	100	A63	85	100
A71	60	50	S1	60	50
A72	60	100	S2	60	100
A73	85	100	S3	85	100

2.3 Statistics of test results

According to the test design in Table 2, which shows the rock core drilling test in the test plan, the specimens after the test are shown in Fig. 2 Real-time monitoring of V, N, M and F is performed during the core drilling tests. Fig. 3

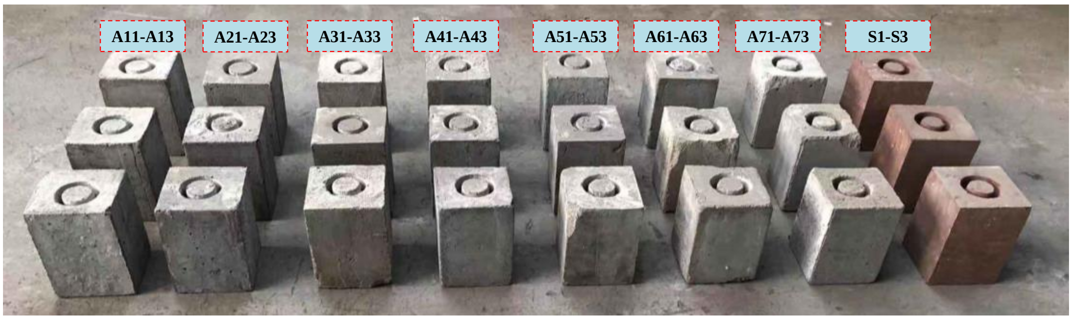

Fig. 2 Digital core drilling test specimen

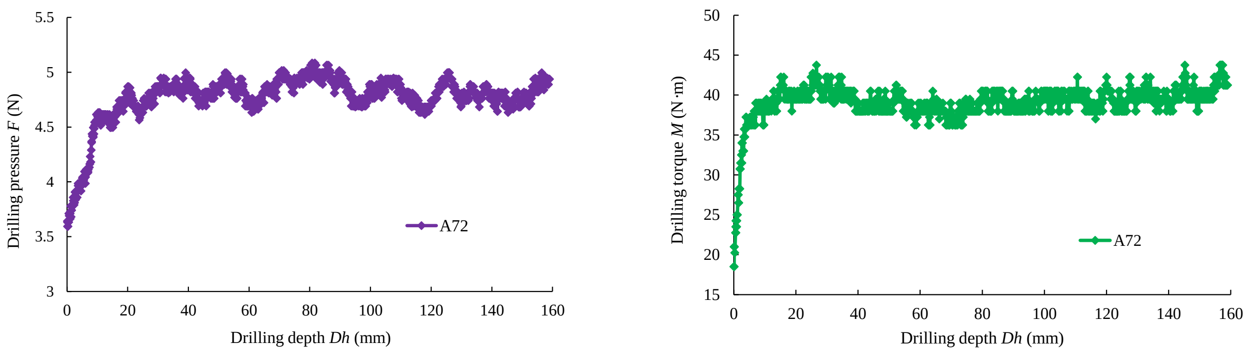

Fig. 3 Dependence of the drilling parameters F and M of specimen A72 on drilling depth

Table 3 Statistics results of drilling parameter monitoring and rock specimen UCS

Specimen type	No. of specimens	V /(mm/min)	N /(r/min)	M /(N·m)	F /kN	UCS /MPa
A1	A11	59.48	50.96	6.24	0.34	7.10
	A12	59.6	100.5	4.27	0.27	7.11
	A13	86.07	100.43	3.57	0.24	7.30
A2	A21	60.02	51.02	8.19	0.27	12.51
	A22	59.63	100.47	8.25	0.43	12.65
	A23	85.3	100.45	3.53	0.22	11.44
A3	A31	59.93	50.95	20.08	0.89	18.37
	A32	60.22	100.37	12.96	0.77	18.87
	A33	85.89	100.41	16.99	0.71	19.95
A4	A41	59.04	51.13	30.94	1.29	24.16
	A42	59.63	100.53	13.75	0.52	24.25
	A43	85.13	100.6	24.8	0.77	21.34
A5	A51	59.42	51.04	35.9	1.24	24.07
	A52	59.23	100.5	23.4	1.29	25.62
	A53	85.11	100.58	28.75	1.14	25.01
A6	A61	59.53	51.03	43.25	1.94	35.22
	A62	59.51	100.57	22.75	1.19	35.87
	A63	85.6	100.44	33.5	1.34	36.05
A7	A71	59.49	50.92	34.5	1.47	29.75
	A72	59.97	100.53	25.53	1.18	37.62
	A73	84.66	100.54	32.45	1.34	33.11
S	S1	60.35	50.79	66.85	2.29	45.69
	S2	61.29	100.33	40.25	1.85	40.26
	S3	83.87	100.29	56.5	2.11	47.36

shows the drilling parameter curve from the test data of specimen A72. *Dh* denotes the drilling depth.

Fig. 3 shows that the trends of the *F* and *M* variations with the drilling depth are similar during the drilling process. Before the drill bit touched the rock, *F* and *M* each had an initial value. As the bit touched the rock and entered further into the rock, *F* and *M* rapidly increased and then stabilized with slight fluctuation around the steady values. Therefore, the test values of *F* or *M* are defined as the average of the stable segment of the *F*-drilling depth curve or *M*-drilling depth curve with the corresponding initial value subtracted. For specimen A72, the average of the stable segment of the *M*-drilling depth curve, M_1, is 39.03 N·m, the initial value of *M*, M_2, is 18.5 N·m, and the test result of the specimen, *M*, is 20.53 N·m ($M = M_1 - M_2$).

The monitoring results of the drilling parameters are statistically analysed using the previously mentioned method, and the laboratory mechanics testing results of the UCS of rock specimens are statistically analysed. The results are listed in Table 3.

3. Energy analysis of rock cutting

To create a quantitative relation between the core drilling parameters and the rock UCS, the cutting-edge force during the drilling process is analysed. The cutting-edge force is shown in Fig. 4: ① the force *T* used to break rocks is applied to all cutting edges of the drill bit by the drilling rig, the force *T* on the combined torque of the drilling center is the torque *M* applied by drilling rig, ② the cutting edges receive resistance P_c from the foremost rocks, ③ the drilling thrust *F* exerted by the drilling rig, and ④ interactive friction *f* between the cutting edge and hole base rock.

Based on the analysis of drill bit cutting edge force, the energies exerted during drilling include the work W_T performed by the work of drilling rock torque *M*, the Work W_F performed by drilling thrust *F* of drilling rock, the energy E_C consumed by breaking rocks by drill cutting, and the energy E_F consumed by the friction between the drill bit and base rock. According to the principle of energy conservation and transformation, a model that analyses the energy of cutting rocks by drilling is established which is shown in Eq. (1):

$$W_M + W_F = E_F + E_C \tag{1}$$

Work W_T performed by the work of drilling rock torque is

$$W_T = 2\pi NtM \tag{2}$$

In the equation, *t* is the time of drilling.

Work W_F performed by drilling thrust is

$$W_F = FVt \tag{3}$$

The energy E_f consumed by the friction between the drilling bit and the base rock is:

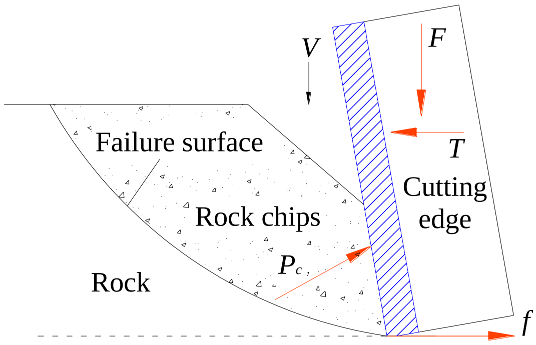

Fig. 4 Stress on the cutting edge of the PDC drill bit

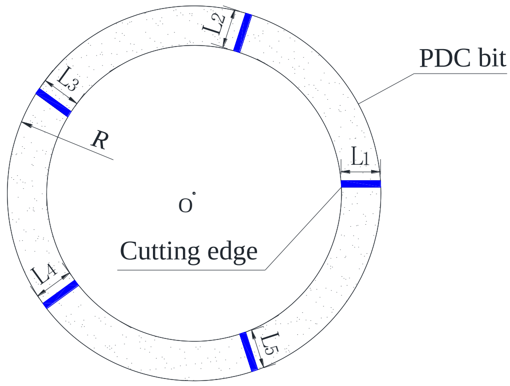

Fig. 5 PDC core bit dedicated to the homemade system

$$E_F = 2\pi Nt\mu F\left[R - \frac{(L_1^2 + L_2^2 + L_3^2 + L_4^2 + L_5^2)}{2(L_1 + L_2 + L_3 + L_4 + L_5)}\right] = 2\pi Nt\mu F\left(R - \frac{l}{2}\right) \tag{4}$$

In this equation, *R* is the radius of the drill bit, *R* = 37.5 mm, L_i is the length of column *i* of the drill bit cutting edge as shown in Fig. 5, and the length of each row of cutting edges is *l* (*l*=9 mm). And μ is the dynamic friction coefficient of the diamond bit cutting edge and the base rock. According to the research results of Yahiaoui *et al.*(2016), the value of μ is set to 0.21.

Substituting Eqs. (2)-(4) into Eq. (1), the energy E_C consumed by the drill bit breaking rocks is:

$$E_C = 2\pi Nt\left[M - \mu FR + \frac{\mu Fl}{2}\right] + FVt \tag{5}$$

In the equation, E_C is the energy consumed in cutting rock in time *t*.

The energy required to drill cut a unit volume of rocks η_c is:

$$\eta_c = \frac{2\pi N\left(M - \mu FR + \frac{\mu Fl}{2}\right) + FV}{\pi R^2 V} \tag{6}$$

Testing the monitoring results of the drilling parameters based on the *V*, *N*, *M* and *F* of the digital drilling test in

Table 3, the cutting breaking energy η_c of all test plans can be calculated by means of Eq. (6), the statistics of the calculation results are displayed in Table 4.

Table 4 η_c calculation results of various specimens

No. of specimens	η_c	No. of specimens	η_c	No. of specimens	η_c	No. of specimens	η_c
A11	4.81	A21	7.70	A31	17.02	A41	27.39
A12	5.81	A22	12.73	A32	18.25	A42	24.45
A13	3.22	A23	3.41	A33	20.23	A43	32.89
A51	33.64	A61	36.78	A71	29.93	S1	61.54
A52	35.19	A62	35.13	A72	41.64	S2	64.28
A53	35.30	A63	40.71	A73	39.43	S3	71.70

4. Quantitative relationship between drilling parameters and rock UCS

4.1 Establishment of the ECD-UCS model

In order to establish the quantitative relationship model between drilling parameters and rock UCS, the methods of regression analysis and support vector machine (SVM) are adopted. The test data of 2 groups of sandstone and 14 groups of cement mortar are selected as the training set to establish the quantitative relationship model. Meanwhile, the test data of the remaining 1 group of sandstone and 7 groups of cement mortar specimens are used as the prediction set to predict rock UCS and verify the validity of the models.

4.1.1 Establishment of the ECD-UCS Model based on regression analysis

The UCS and η_c of each specimen are subjected to a linear regression analysis, and the regression prediction model is established (Fig. 6).

Fig. 6 shows that the coefficient of determination R^2 is 0.9289, which is acceptable. Based on the best-fitting curve, the relationship model of η_c and the rock UCS is established:

$$R_c = 0.6046\eta_c + 7.3051 \quad (7)$$

In the equation, R_c is the predicted value of the rock UCS.

Substituting Eq. (6) into Eq. (7), the ECD-UCS model is obtained:

$$R_c = 0.6046 \times \frac{2\pi N\left(M - \mu FR + \dfrac{\mu Fl}{2}\right) + FV}{\pi R^2 V} + 7.3051 \quad (8)$$

4.1.2 Establishment of the ECD-UCS model based on SVM

Support vector machines (SVM) (Cristianini and Shawe 2000, Burges 1998,Vapnik 1995) are general machine learning methods that are developed based on the VC-dimension theory and the structural risk minimization principle in statistical learning. The SVM is primarily

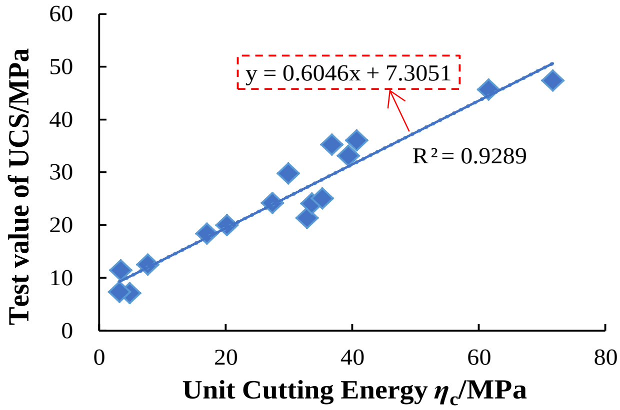

Fig. 6 Cutting energy per unit volume of rock removed-UCS relationship fitting curve

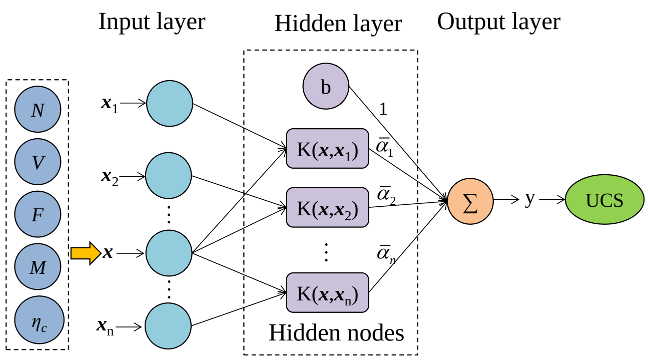

Fig. 7 Diagram that shows the construction of the ECD-UCS model based on SVM

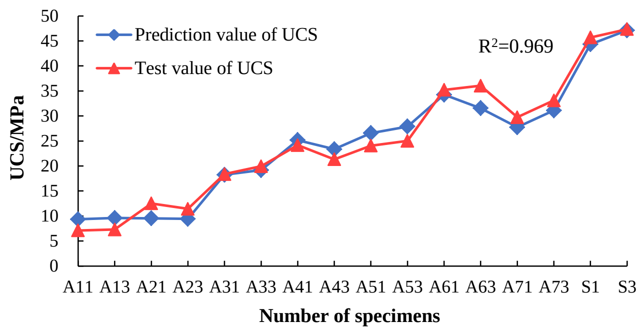

Fig. 8 Comparison between the predicted UCS values in the training set and the UCS values obtained by the uniaxial compression test

employed in pattern recognition, classification and regression. The successful application of SVM in multiple geotechnical engineering prediction problems (Xu 2017, Zhang *et al.* 2016, Huang *et al.* 2009) indicates its effectiveness and broad applicability in the construction of nonlinear models.

The ECD-UCS model is established by the method of SVM. The kernel function of this paper is the radial basis function (RBF) kernel, and the equation is expressed as follows:

$$K(x_i, x_k) = \exp(-\gamma \|x_i - x_k\|^2), \quad \gamma > 0 \quad (9)$$

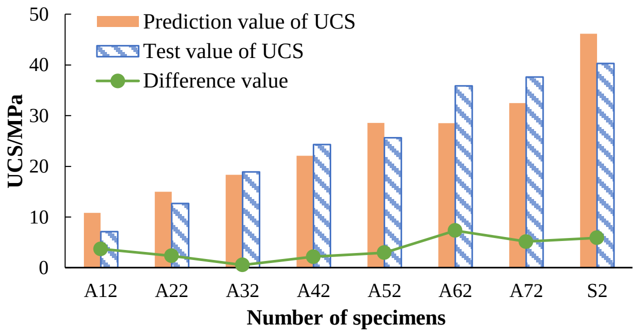

Fig. 9 Analysis of the predictive ability of the regression analysis-based model

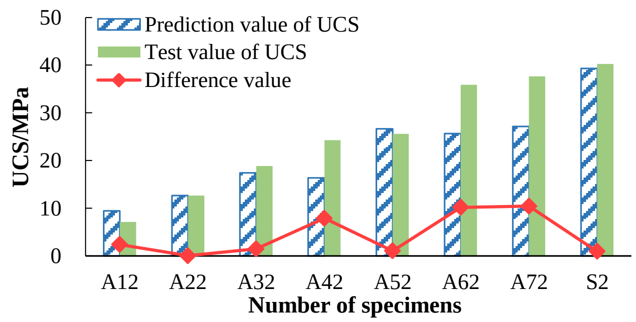

Fig. 10 Analysis of the predictive ability of the SVM-based model

Table 5 Relative difference between the predicted UCS values and the tested UCS values

No. of specimens	Predicted UCS value /MPa		Tested UCS value /MPa	δ/MPa	
	Regression analysis method	SVM method		Regression analysis method	SVM method
A12	10.82	9.49	7.11	3.71	2.38
A22	14.99	12.67	12.64	2.35	0.03
A32	18.33	17.41	18.87	0.53	1.46
A42	22.08	16.36	24.25	2.16	7.89
A52	28.57	26.66	25.62	2.95	1.04
A62	28.54	25.67	35.86	7.32	10.19
A72	32.47	27.19	37.62	5.14	10.43
S2	46.16	39.31	40.26	5.90	0.95

The prediction accuracy of the model depends on the selection of the parameters C, γ and ε when using this kernel function. Model parameters such as C with the search range 2^{-8}~2^{8}, kernel parameter γ with 2^{-8}~2^{8}, ε with 0.1 are selected for establishing the SVM model. This study employed a grid search and 5-fold cross-validation (Barzegar *et al.* 2016, Wan *et al.* 2010) to select the best C, γ and ε values. Based on the training set data, the optimal C, γ and ε values are 48.5029, 0.0359 and 0.10, respectively, and the ECD-UCS model is established. Fig. 7 shows the corresponding data points (x_i, y_i) of any specimen, where x_i is a 5-dimensional real input vector, including N, V, F, M and η_c, and y_i represents the specimen's UCS measured in the uniaxial compression test.

Fig. 8 shows that the predicted UCS values are similar to the test values, and the coefficient of determination R^2 is 0.969, which indicates that the ECD-UCS model that is established using SVM has a high degree of fitting.

4.2 ECD-UCS Model predictive capability analysis

Based on the selected verification set, the predictive abilities of the ECD-UCS model established by regression analysis and SVM are comparatively analysed (Figs. 9-10). In order to quantitatively evaluate the predictive abilities of the ECD-UCS model, an index for the relative difference of the UCS, $\delta = |R_p - R_t|$, is established, where R_p (referred to as the predicted value) is the UCS value predicted by the ECD-UCS model, and R_t (referred to as the test value) is the UCS value measured by the uniaxial compression test. The relative error indicators of the UCS values in the prediction set are listed in Table 5.

From Figs. 9 and 10 and Table 5, the mean value of δ for the regression analysis-based ECD-UCS model is 3.76 MPa, and the standard deviation is 2.08 MPa. The mean value of δ for the SVM-based ECD-UCS model is 4.30 MPa, and the standard deviation is 4.14 MPa. The predicted and test values of UCS are relatively similar, which indicates that both ECD-UCS models have excellent prediction abilities. The deviation of the value predicted by the regression analysis-based ECD-UCS model from the test value is small, and the δ curve is relatively flat, which indicates that the regression analysis-based ECD-UCS model has superior prediction results that are more stable and accurate.

4.3 Establishment of rock UCS prediction method

Based on the constructed ECD-UCS model, the energy analysis-based rock drilling method for the prediction of UCS is proposed. The procedure is as follows:

(1) The rock mass digital core drilling test is conducted based on a surrounding rock digital drilling test system. During drilling, the drilling parameters V, N, M and F in the entire drilling range are monitored in real time.

(2) Based on the ECD-UCS model established by the above, the surrounding rock UCS distribution law in the entire drilling range is obtained via monitored drilling parameter.

At the same time of digital core drilling, standard rock mechanics tests are carried out on the core samples obtained, and the standard values of rock UCS laboratory test are obtained, which is compared with the rock UCS forecast by the ECD-UCS model for verification. The ECD-UCS model is continuously modified to construct a real-time in situ rock UCS forecast method with an extensive range of applications.

5. Conclusions

• Using the self-developed multi-function digital rock drilling and testing system and the digital drilling core bit dedicated to the system, digital drilling tests of rock specimens with different strengths is performed, and the drilling parameters *V*, *N*, *M* and *F*, which are monitored during the drilling process, are obtained. The dependence of the drilling torque *M* and the drilling thrust *F* on the drilling depth is analysed.

• An analysis of rock cutting energy is performed to determine the energy consumed by the drill bit per unit volume of rock removed, η_c. The relationship equation of the drilling parameters and unit rock cutting energy η_c are obtained. Two quantitative models for the relationship of the drilling parameters and rock UCS are separately established by the methods of regression analysis and SVM, based on the core drilling testing results of test specimens with the strength ranges from 7.10 to 47.36 MPa.

• The prediction abilities of the ECD-UCS models are compared. The mean value of δ for the regression analysis-based ECD-UCS model is 3.76 MPa, and the standard deviation is 2.08 MPa. The mean value of δ for the SVM-based ECD-UCS model is 4.30 MPa, and the standard deviation is 4.14 MPa. Both models have excellent prediction abilities for the rock UCS. The regression analysis-based ECD-UCS model has a more stable predictive ability.

• Based on the previously mentioned results, the energy analysis-based rock drilling method for the prediction of the uniaxial compressive strength, which can effectively achieve rapid and convenient in situ prediction of rock UCS is proposed. The authors will conduct extensive digital core drilling tests for different types of engineering rock bodies and continuously validate and modify the ECD-UCS model to provide accurate basic parameters for support design and the analysis and timely optimization of surrounding rock stability for underground projects.

Acknowledgments

This work was supported by the Natural Science Foundation of China (Nos. 51874188, 51704125 and 51927807), the Major Scientific and Technological Innovation Project of Shandong Province, China (Nos. 2019SDZY04 and 2018GGX109001), the Project of Shandong Province Higher Educational Youth Innovation Science and Technology Program, China (No. 2019KJG013).

References

Arora, S. and Mishra, B. (2015), “Investigation of the failure mode of shale rocks in biaxial and triaxial compression tests”, *Int. J. Rock Mech. Min. Sci.*, **79**, 109-123. https://doi.org/10.1016/j.ijrmms.2015.08.014.

Barzegar, R., Sattarpour, M., Nikudel, M.R. and Moghaddam, A.A. (2016), “Comparative evaluation of artificial intelligence models for prediction of uniaxial compressive strength of travertine rocks, Case study: Azarshahr area, NW Iran”, *Model Earth Syst. Environ.*, **2**(2), 1-13. https://doi.org/10.1007/s40808-016-0132-8.

Burges, C.J.C. (1998), “A tutorial on support vector machines for pattern recognition”, *Knowledge Discovery Data Min.*, **2**(2), 121-167. https://doi.org/10.1023/A:1009715923555.

Chai, Z.Y., Bai, J.B. and Sun, Y.H. (2019), “Change of pore structure and uniaxial compressive strength of sandstone under electrochemical coupling”, *Geomech. Eng.*, **17**(2), 157-164. https://doi.org/10.12989/gae.2019.17.2.157.

Cristianini, N. and Shawe-Taylor, J. (2000), *Support Vector Machines and Other Kernel-Based Learning Methods*, Cambridge University Press, Oxford city, U.K.

Ghosh, R., Gustafson, A. and Schunnesson, H. (2018), “Development of a geological model for chargeability assessment of borehole using drill monitoring technique”, *Int. J. Rock Mech. Min. Sci.*, **109**, 9-18. https://doi.org/10.1016/j.ijrmms.2018.06.015.

Heidari, M., Khanlari, G.R., Kaveh, M.T. and Kargarian, S. (2012), “Predicting the uniaxial compressive and tensile strengths of gypsum rock by point load testing”, *Rock Mech. Rock Eng.*, **45**(2), 265-273. https://doi.org/10.1007/s00603-012-0264-8.

Huang, W.Y., Tong, M.M. and Ren, Z.H. (2009), “Nonlinear combination forecast of gas emission amount based on SVM”, *J. China U. Min. Technol.*, **38**(2), 234-239. https://doi.org/10.3321/j.issn:1000-1964.2009.02.017.

Kahraman, S. and Yeken, T. (2010), “Electrical resistivity measurement to predict uniaxial compressive and tensile strength of igneous rocks”, *B. Mater. Sci.*, **33**(6), 731-735. https://doi.org/10.1007/s12034-011-0137-x.

Kalantari, S., Hashemolhosseini, H. and Baghbanan, A. (2018), “Estimating rock strength parameters using drilling data”, *Int. J. Rock Mech. Min. Sci.*, **104**, 45-52. https://doi.org/10.1016/j.ijrmms.2018.02.013.

Kilic, A. and Teymen, A. (2008), “Determination of mechanical properties of rocks using simple methods”, *B. Eng. Geol. Environ.*, **67**, 237-244. https://doi.org/10.1007/s10064-008-0128-3.

Kumar, B.R., Vardhan, H. and Govindaraj, M. (2011), “Prediction of uniaxial compressive strength, tensile strength and porosity of sedimentary rocks using sound level produced during rotary drilling”, *Rock Mech. Rock Eng.*, **44**(5), 613-620. https://doi.org/10.1007/s00603-011-0160-7.

Kun, M. and Onargan, T. (2013), “Influence of the fault zone in shallow tunneling: A case study of Izmir Metro Tunnel”, *Tunn. Undergr. Sp. Tech.*, **33**(1), 34-45. https://doi.org/10.1016/j.tust.2012.06.016.

Langford, J.C., Vlachopoulos, N. and Diederichs, M.S. (2016), “Revisiting support optimization at the Driskos tunnel using a quantitative risk approach”, *J. Rock Mech. Eng.*, **8**(2), 147-163. https://doi.org/10.1016/j.jrmge.2015.11.003.

Lei, G.F., Liu, Q.S., Peng, X.X. and Wei, L. (2020), “Experimental study on mechanical properties of fractured rock mass under different anchoring modes”, *Eur. J. Environ. Civ. Eng.*, **24**(7), 931-948. https://doi.org/10.1080/19648189.2018.1429321.

Li, W. and Tan, Z.Y. (2016), “Prediction of uniaxial compressive strength of rock based on P-wave modulus”, *Rock Soil Mech.*, **37**(S2), 381-387 (in Chinese). https://doi.org/10.16285/j.rsm.2016.S2.049.

Li, Y., Zhou, H., Zhang, L., Zhu, W.S., Li, S.C. and Liu, J. (2016), “Experimental and numerical investigations on mechanical property and reinforcement effect of bolted jointed rock mass”, *Constr. Build. Mater.*, **126**, 843-856. https://doi.org/10.1016/j.conbuildmat.2016.09.100.

Momeni, E., Armaghani, D.J., Hajihassani, M. and Amin, M.F.M. (2015), “Prediction of uniaxial compressive strength of rock samples using hybrid particle swarm optimization-based artificial neural networks”, *Measurement*, **60**, 50-63. https://doi.org/10.1016/j.measurement.2014.09.075.

Mostofi, M., Rasouli, V. and Mawuli, E. (2011), “An estimation of rock strength using a drilling performance model: A case study in blacktip field, Australia”, *Rock Mech. Rock Eng.*, **44**(3), 305-

316. https://doi.org/10.1007/s00603-011-0142-9.
Munoz, H., Taheri, A. and Chanda, E.K. (2016), "Rock drilling performance evaluation by an energy dissipation based rock brittleness index", *Rock Mech. Rock Eng.*, **49**(8), 3343-3355. https://doi.org/10.1007/s00603-016-0986-0.
Qian, D.Y., Zhang, N., Pan, D.J., Xie, Z.Z., Shimada, H., Wang, Y., Zhang, C.H. and Zhang, N.C. (2017), "Stability of deep underground openings through large fault zones in argillaceous rock", *Sustainability*, **9**(12), 2153. https://doi.org/10.3390/su9112153.
Su, H.J., Jing, H.W., Zhao, H.H., Yu, L.Y. and Wang, Y.C. (2017), "Strength degradation and anchoring behavior of rock mass in the fault fracture zone", *Environ. Earth Sci.*, **76**(4), 179. https://doi.org/10.1007/s12665-017-6501-4.
Vapnik V.N. (1995), *The Nature of Statistical Learning Theory*, Springer, New York, U.S.A.
Vyacheslav, P. (2018), "Applicability of exponential stress-strain models for carbonate rocks", *Geomech. Eng.*, **15**(3), 915-929. https://doi.org/10.12989/gae.2018.15.3.919.
Wan, Z., Dong, H. and Liu, B.C. (2010), "On choice of hyper-parameters of support vector machines for time series regression and prediction with orthogonal design", *Rock Soil Mech.*, **32**(2), 503-508, 515 (in Chinese). https://doi.org/10.16285/j.rsm.2010.02.007.
Wang, Q., Pan, R., Jiang, B., Li, S.C., He, M.C., Sun, H.B., Wang, L., Qin, Q., Yu, H.C. and Luan, Y.C. (2017), "Study on failure mechanism of roadway with soft rock in deep coal mine and confined concrete support system", *Eng. Fail. Anal.*, **81**, 155-177. https://doi.org/10.1016/j.engfailanal.2017.08.003.
Wang, Q., Gao, H.K., Jiang, Z.H., Li, S.C. and Jiang, B. (2020a), "Development and application of a surrounding rock digital drilling test system of underground engineering", *Chin. Rock Mech. Eng.*, **39**(2), 301-310 (in Chinese). https://doi.org/10.13722/j.cnki.jrme.2019.0744.
Wang, Q., He, M.C., Yang, J., Gao, H.K., Jiang, B. and Yu H.C. (2018a), "Study of a no-pillar mining technique with automatically formed gob-side entry retaining for longwall mining in coal mines", *Int. J. Rock Mech. Min. Sci.*, **110**, 1-8. https://doi.org/10.1016/j.ijrmms.2018.07.005.
Wang, Q., Jiang, B., Pan, R., Li, S.C., He, M.C., Sun, H.B., Qin, Q., Yu, H.C. and Luan, Y.C. (2018b), "Failure mechanism of surrounding rock with high stress and confined concrete support system", *Int. Ji. Rock Mech. Min. Sci.*, **102**, 89-100. https://doi.org/10.1016/j.ijrmms.2018.01.020.
Wang, Q., Jiang, Z.H., Jiang, B., Gao, H.K., Huang, Y.B. and Zhang, P. (2020b), "Research on an automatic roadway formation method in deep mining areas by roof cutting with high-strength bolt-grouting", *Int. J. Rock Mech. Min. Sci.*, **128**, 104264. https://doi.org/10.1016/j.ijrmms.2020.104264.
Wang, Y. and Aladejare, A.E. (2016), "Bayesian characterization of correlation between uniaxial compressive strength and Young's modulus of rock", *Int. J. Rock Mech. Min. Sci.*, **85**, 10-19. https://doi.org/10.1016/j.ijrmms.2016.02.010.
Wang. Q., Gao. H.K., Yu. H.C., Jiang. B. and Liu. B.H. (2019), "Method for measuring rock mass characteristics and evaluating the grouting-reinforced effect based on digital drilling", *Rock Mech. Rock Eng.*, **52**(3), 841-851. https://doi.org/10.1007/s00603-018-1624-9.
Wu, X., Jiang, Y. and Li, B. (2018), "Influence of joint roughness on the shear behaviour of fully encapsulated rock bolt", *Rock Mech. Rock Eng.*, **51**(3), 953-959. https://doi.org/10.1007/s00603-017-1365-1.
Xu, J.C., Ren, Q.W. and Shen, Z.Z. (2017), "Sensitivity analysis of the influencing factors of slope stability based on LS-SVM", *Geomech. Eng.*, **13**(3), 447-458. https://doi.org/10.12989/gae.2017.13.3.447.
Yahiaoui, M., Paris, J.Y., Delbé, K., Denape, J., Gerbaud, L. and Dourfaye, A. (2016), "Independent analyses of cutting and friction forces applied on a single polycrystalline diamond compact cutter", *Int. J. Rock Mech. Min. Sci.*, **85**, 20-26. https://doi.org/10.1016/j.ijrmms.2016.03.002.
Yaşar, E., Ranjith, P.G. and Viete, D.R. (2011), "An experimental investigation into the drilling and physico-mechanical properties of a rock-like brittle material", *J. Petrol. Sci. Eng.*, **76**, 185-193. https://doi.org/10.1016/j.petrol.2011.01.011.
Yong, R., Ye, J., Li, B. and Du, S.G. (2018), "Determining the maximum sampling interval in rock joint roughness measurements using Fourier series", *Int. J. Rock Mech. Min. Sci.*, **101**, 78-88. https://doi.org/10.1016/j.ijrmms.2017.11.008.
Yu, J., Liu, GY., Cai, Y.Y., Zhou, J.F., Liu, S.Y. and Tu, B.X. (2020), "Time-dependent deformation mechanism for swelling soft-rock tunnels in coal mines and its mathematical deduction", *Int. J. Geomech.*, **20**(3), 04019186. https://doi.org/10.1061/(asce)gm.1943-5622.0001594.
Zhang, B., Li, S.C., Yang, X.Y., Xia, K.W., Liu, J.Y., Guo, S. and Wang, S.G. (2019), "The coalescence and strength of rock-like materials containing two aligned X-type flaws under uniaxial compression", *Geomech. Eng.*, **17**(1), 47-56. https://doi.org/10.12989/gae.2019.17.1.047.
Zhang, B., Li, S.C., Yang, X.Y., Zhang, D.F., Wang, Q., Cai, W., Yang, C.X. and Deng, Z.Q. (2015), "Mechanical property of rock-like material with intersecting multi-flaws under uniaxial compression", *Chin. J. Rock Mech. Eng.*, **34**(9), 1777-1785 (in Chinese). https://doi.org/10.13722/j.cnki.jrme.2014.0876.
Zhang, C.S., Ji, J., Gui, Y.L., Kodikara, J., Yang, S.Q. and He, L. (2016), "Evaluation of soil-concrete interface shear strength based on LS-SVM", *Geomech. Eng.*, **11**(3), 361-372. https://doi.org/110.12989/gae.2016.11.3.361.
Zhao, X.G., Cai, M., Wang, J. and Li, P.F. (2015), "Strength comparison between cylindrical and prism specimens of Beishan granite under uniaxial compression", *Int. J. Rock Mech. Min. Sci.*, **766**, 10-17. https://doi.org/10.1016/j.ijrmms.2015.02.009.
Zhou, Y., Zhang, W., Gamwo, I. and Lin, J.S. (2017), "Mechanical specific energy versus depth of cut in rock cutting and drilling", *Int. J. Rock Mech. Min. Sci.*, **100**, 287-297. https://doi.org/10.1016/j.ijrmms.2017.11.004.

JS